GEOPHYSICAL RESEARCH LETTERS, VOL. 24, NO.8, PAGES 999-1002, APRIL 15, 1997

Initial comparison of POLAR UVI and Sondrestrom IS radar estimates for auroral electron energy flux

Richard A. Doe [1], John D. Kelly [1], Dirk Lummerzheim [2], George K. Parks[3], Mitchell J. Brittnacher[3], Glynn A. Germany[4], and James Spann[5]

Abstract. Calibrated images from the POLAR satellite ultraviolet imager (UVI) in the 165.5 to 174.5 nm portion of the N_2 Lyman-Birge-Hopfield band (LBH-long) can be used to estimate the energy flux (F_E) of auroral electrons precipitating into the high-latitude ionosphere. Similarly, electron density profiles, as measured by ground-based incoherent-scatter radar, can be used to estimate F_E and mean energy (E_0) by solving a system of linear equations relating the *E*-region ionization rate profile to a family of monoenergetic ion production profiles. A coordinated POLAR/Sondrestrom radar experiment, designed as an initial comparison of POLAR UVI and ground-based estimates of F_E for a stable auroral arc, was executed during a POLAR apogee on May 20, 1996 at the Sondrestrom radar facility (lat. 66.99° N, long. 50.95° W). Reconstructed energy distributions, based on radar-measured N_e profiles, indicate an approximately 2 keV Maxwellian source with an energy flux of from 6.4 to 14 mW m^{-2}. LBH-long images, binned over 0.5° of latitude and 1.0° of longitude, were used to derive energy flux as well. The UVI-derived F_E time history agrees favorably with radar estimates both in absolute magnitude and in the trend for this period. This experiment suggests that reliable estimates for the precipitating electron source energy and its ionospheric response can be derived from either ground-based radar or POLAR UVI images during summertime conditions.

1. Introduction

Effective application of existing electrodynamic models as space weather diagnostics will require high time resolution ionospheric parameters from both ground-based and orbital platforms [*Behnke et al.,* 1995]. In this role, satellite UV and visible imaging diagnostics are increasingly being used to estimate the ionospheric response to energetic auroral precipitation. For example, single wavelength images from the DE-1 satellite have been used to relate UV brightness to ground-based measurements of ionospheric conductance [*Robinson et al.,* 1989]. Pairs of UV/visible images from polar orbiting satellites have been used to characterize the energetics of the precipitating electron source on the nightside [*Lummerzheim et al.,* 1991; *Robinson et al.,* 1992].

[1]SRI International, Menlo Park, California
[2]University of Alaska, Fairbanks, Alaska
[3]University of Washington, Seattle, Washington
[4]University of Alabama, Huntsville, Alabama
[5]Marshall Space Flight Center, Huntsville, Alabama

Paper number 97GL00376.
0094-8534/97/97GL-00376$05.00

The key to successful analysis of this type is to select a pair of wavelengths that allow the extraction of both mean energy and energy flux from nearly simultaneous images. An electron transport/degradation model can then be invoked to recover estimates for $N_e(z)$ and conductivity. As a complement to such analysis, ground-based incoherent-scatter (IS) radar can measure $N_e(z)$ directly and can provide an estimate for the source energy distribution by carefully analyzing the shape of the *E*-region ionization profile [*Vondrak and Baron,* 1977; *Brekke et al.,* 1989].

Prior attempts to compare such satellite/ground-based ionospheric measurements have purposely avoided sunlit measurements. Visible imagers on the DE-1 and the Polar BEAR satellite, for example, were incapable of dayside measurement due to scattered sunlight contamination of the 557.7 nm and 391.4 nm filters, respectively. DE-1 UV filters were sufficiently broad so that the dayglow contribution was difficult to remove from UV images as well. Analysis of ground-based IS radar measurements from such sunlit periods is also complicated as the specific shape of N_e profiles results from a contribution of auroral impact and photoionization processes.

This paper describes how the capabilities of the new POLAR satellite and new Sondrestrom radar analysis techniques can both provide estimates for F_E during summertime conditions. The POLAR ultraviolet imager (UVI) has been specifically designed to provide sunlit estimates of auroral F_E by providing (N_2) images in the LBH-long band [*Torr et al.,* 1995]. A technique to extract F_E from IS radar measurements of $N_e(z)$, first described by *Brekke et al.* [1989], has recently been merged with an ionospheric simulation [*Min et al.,* 1993] in order to analyze summertime auroral data. As a first step in exploiting the capability of both POLAR UVI and Sondrestrom radar to measure auroral energy flux accurately, an experiment was designed to cross-compare estimates of F_E for a stable arc observed at the polarward boundary of the auroral oval on May 20, 1996.

2. Measurement of Auroral Energy Flux

2.1. POLAR UVI Technique

The POLAR satellite UVI experiment was designed to assess the state of auroral ionospheric emission during periods with significant solar UV scattering. The UVI instrument has oxygen filters, two filters in the N_2 LBH band, and a broadband filter for scattered solar UV. The two N_2 LBH filters are selected so that one observes in the wavelength range where the emission experiences extinction from Schuman-Runge absorption (LBH-short), while the other (LBH-long) is centered at longer wavelengths, where absorption plays a minor role. This LBH-long band emission, with a peak emission altitude of 120 km [*Stolarski*, 1968], is therefore relatively insensitive to the characteristic energy of the precipitating electrons and is dependent primarily on the total energy flux. The technique to extract F_E from N_2 LBH-long band images thus reduces to correcting the images for flat field, noise, and contributions due to UV dayglow. Pre-flight UVI calibration data and the ionospheric model of *Min et al.* [1993] allow such photometrically corrected LBH-long images to be scaled from brightness in Raleighs to energy flux in mW m^{-2} with an uncertainty no greater than ±30%.

2.2. Ground-Based Technique

IS radar techniques for reconstructing the precipitating electron energy distribution start with the assumption that molecular ion recombination dominates other loss and transport processes in the E region. Thus, at altitudes less than approximately 200 km, an ion production profile can be derived from the square of the radar-measured electron density profile:

$$q(z) = \alpha(z) N_e(z)^2, \tag{1}$$

where $\alpha(z)$ is the height-dependent effective recombination coefficient given by *Vickrey et al.* [1982]. In order to isolate the ionization effects solely due to the impact of auroral electrons, we must adjust the $q(z)$ profile for the effects of solar photoionization. We have determined this solar contribution by running the time-dependent ionospheric model of *Min et al.* [1993], calculating an effective ionization rate profile based on the resultant solar $N_e(z)$, and subtracting the result from the radar-derived $q(z)$. This model solves an electron transport equation, continuity equations for all major and minor ions, and the energy equation for electrons and ions to obtain a description of the auroral ionosphere. In order to simulate the effect of solar photoionization, this model was run without auroral input for a 1-h period prior to the start time of this experiment.

An auroral ionization rate profile results from the superposition of contributions from all energies spanned by the auroral source distribution. *Brekke et al.* [1989] introduce a compact matrix notation for such a composite ionization rate profile:

$$\mathbf{q} = \overleftrightarrow{\mathbf{Q}} \cdot \phi(\mathbf{E}, \mu) \boldsymbol{\Delta} \mathbf{E} \boldsymbol{\Delta} \mu, \tag{2}$$

where $\mathbf{q}$ is the measured ionization rate profile, $\overleftrightarrow{\mathbf{Q}}$ is a tensor of monoenergetic ionization rate altitude profiles versus discrete energies, $\phi(E,\mu)$ is the number flux in energy bin ΔE over an angle range $\Delta\mu$ in units of cm^{-2} s^{-1} sr^{-1}, and μ is cosine of pitch angle. Thus the desired energy distribution $\phi(E,\mu)$ can be derived by simply solving a system of linear equations.

The $\overleftrightarrow{\mathbf{Q}}$ tensor is constructed by solving an ionization expression [*Rees*, 1989, and references within] over a range of altitudes (200 km to 84 km) and energies (288 eV to 44 keV):

$$Q(E,z) = \left(\frac{\phi_0}{\Delta\epsilon_{ion}}\right)\left(\frac{E\rho(z)\Lambda(E,z)}{R(E)}\right), \tag{3}$$

where the number flux ϕ_0 is fixed at 10^8 cm^{-2} s^{-1} sr^{-1}, $\Delta\epsilon_{ion}$ is energy loss per ion pair (35 eV), $\rho(z)$ is the MSIS-90 mass density function, $\Lambda(E,z)$ is the normalized energy deposition distribution function for a unidirectional beam [*Barrett and Hays*, 1976], and $R(E)$ is the effective stopping range. Equation (2) is solved using single value decomposition methods [*Press et al.*, 1986] suitably constrained so that $\phi(E,\mu)$ is forced to be non-negative. The total downward energy flux F_E is then found by integrating $E\phi(E,\mu)$ over all energies and over all pitch angles in the downward unit hemisphere:

$$F_E = 2\pi \int_0^\infty \int_{-1}^0 E\phi(E,\mu)\, \mu d\mu\, dE. \tag{4}$$

In a similar manner, total number flux F_N is found by integrating $\phi(E,\mu)$ over all energies and pitch angles. The characteristic energy E_0 is defined as half the ratio of F_E to F_N.

3. Experiment Description

The POLAR satellite is currently in a 1.85 × 8.94 R_e 17.5-h orbit and the apogee period for this experiment ran from 1400 UT on May 19, 1996, to 0300 UT on May 20, 1996. During this period, the UVI instrument was configured to record two sequential LBH-long images interleaved with a series of four sequential LBH-short images. Individual LBH-long images were integrated for approximately 36 s and the interval between LBH-long image pairs was approximately 260 s.

During this period, the Sondrestrom IS radar [*Kelly et al.*, 1995] was mostly scanned in the plane of the magnetic meridian with an occasional pause to dwell at magnetic zenith. The transmitted waveform (A16) was a 16-baud, alternating code with 32 different coded pulses, each with a baud length of 20 μs. The range resolution of this mode, subject to the recovery of a sufficiently large signal-to-noise ratio (SNR), is 3 km in the E region. This coded pulse was interleaved with a 320-μs long pulse that was used to recover data when the SNR was insufficient for reliable A16 analysis.

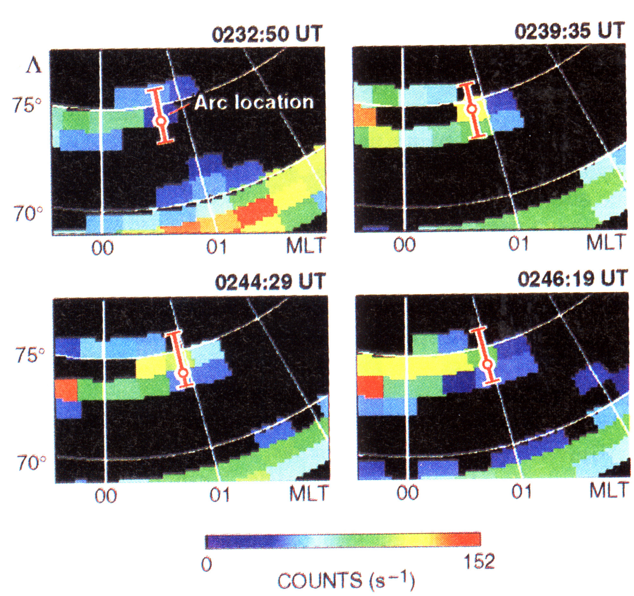

Plate 1. POLAR N_2 LBH-band images during May 20,1996 apogee. The instantaneous location of the arc as determined by the Sondrestrom IS radar is indicated with a small circle.

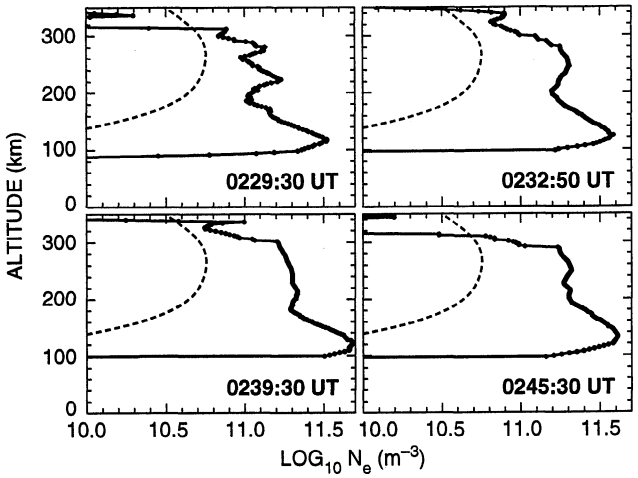

Figure 1. Four sequential N_e profiles measured during the arc event. The dashed line represents the solar photoionization contribution to the profile from the *Min et al.* [1993] model.

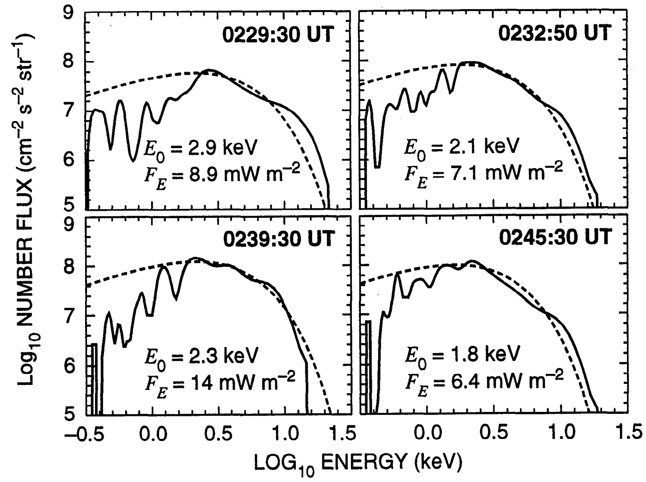

Figure 2. Energy distributions corresponding to the four profiles shown in Figure 1. Characteristic energy and energy flux was calculated for each distribution as described in the text. Maxwellian fits have been shown for reference.

The auroral oval was quite dynamic on May 20, 1996. A series of onsets were observed in the evening sector from 0033 UT to 0051 UT, followed by a main expansion at 0051 UT and an extended recovery phase from 0110 UT to 0250 UT. During the period from 0229:30 UT to 0245:30 UT a late-recovery phase arc was detected in both POLAR UVI LBH images and in Sondrestrom elevation scans. This period was selected as the arc was morphologically stable and was observed at a high elevation angle above the IS radar. Such a stable arc allows the acquisition of high-fidelity *E*-region N_e profiles that are minimally free of smearing due to horizontal arc motion.

Plate 1 shows the detailed juxtaposition of LBH short and long band images with the radar location of the arc (as determined by nearly simultaneous scans). This plate demonstrates that the radar and UVI imager were measureing the same common volume. Figure 1 shows four electron density profiles extracted from elevation scans during this period. Structure in the ionization profile above 200 km is most probably due to *F*-region ionization advecting from the dayside. The photoionization profile from the aforementioned 1-h simulation is indicated with a dashed line.

4. Analysis and Discussion

Once the profiles shown in Figure 1 have been converted to $q(z)$ profiles (corrected for the effects of solar photoionization), energy analysis procedes directly from the matrix method described in Section 2.2. Figure 2 shows the resultant energy distributions for these four N_e profiles. Values of F_E and E_0 for each distribution have been calculated as well. The similarity of the overall shape and value of E_0 for these four energy distributions suggests that the arc was energetically as well as morphologically stable throughout this period.

The energy distributions shown in Figure 2 are well represented by Maxwellian distributions. Maxwellian fits, shown as dashed lines, are most accurate for energies above approximately 2 keV, suggesting that perhaps the source population was accelerated through a small (0.5 kV) potential. Even without the inclusion of an accelerating potential, the values of F_E calculated for the Maxwellian fits are accurate to within 5% of the actual energy flux for all four distributions. The observation of such distributions validates the suggestion of *Robinson et al.* [1992] that diffuse boundary arcs are more likely to be due to Maxwellian sources, in contrast to structured auroral zone arcs, which are best fit with Gaussian sources.

The time history of F_E derived from the POLAR UVI LBH-long images, shown in Figure 3, has been overlain with F_E estimates from the IS radar data analysis. The size of the UVI PIXEL bin is lat 0.5° × long.1° and the bin spans the geomagnetic location of the arc. Two curves are shown for the UVI data — one indicates the time history for F_E base on the brightest (maximum) PIXEL in the bin and the other indicates the time history for F_E based on the mean brightness in the bin. Overall, this plot shows good agreement in both the magnitude and the time evolution of energy flux for POLAR UVI and Sondrestrom techniques.

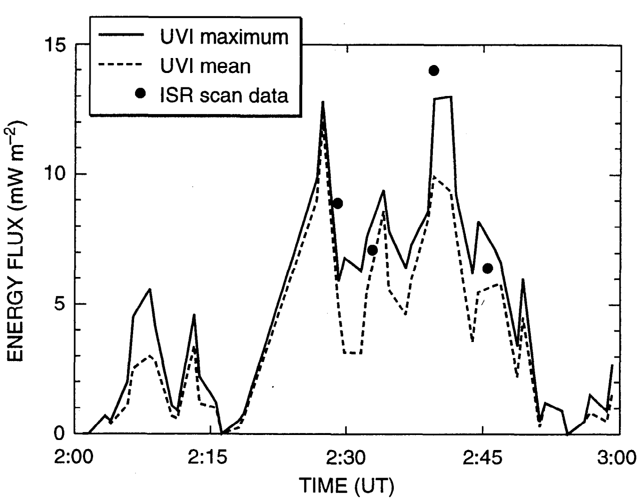

Figure 3. Time history of energy flux from UVI and IS radar data.

5. Conclusion

This experiment was designed to cross-compare IS radar and preliminary POLAR UVI energy flux estimates for a stable auroral boundary arc. Detailed IS radar analysis of this arc indicates that the magnetospheric source distribution has the form of an accelerated Maxwellian approximately 2 to 3 keV in width with energy flux from 6.4 to 14.0 mW m^{-2}. Total energy flux from IS radar measurements agree to within the ±30% uncertainty of the POLAR UVI F_E estimates over a 16-min period. Such close agreement suggests that both POLAR UVI LBH-long images and Sondrestrom IS radar measurements are reliable diagnostics for the energy flux of the precipitating electron population and that such measurements can be made during summertime conditions. Future comparisons of satellite/ground-based E_0 estimates, subject to final UVI LBH-short image calibration, will initiate significant refinements in operational techniques used to derive N_e and conductance parameters solely from POLAR UVI data.

Acknowledgments. We are grateful to Craig Heinselman for fruitful discussions on state-of-the-art techniques to implement the CARD algorithm. This research was supported at SRI by NASA grant NAS5-31185 and was supported at University of Alaska by NASA grant NAG5-1097.

References

Barrett, J. L., and P. B. Hays, Spatial distribution of energy deposited in nitrogen by electrons, *J. Chem. Phys., 64*, 743, 1976.

Behnke, R. A., T. F. Tascione, E. Hildner, W. Cliffswallow, R. M. Robinson, N. E. Cobb, A. W. Green, S. Basu, O. de la Beaujardière, and R. L. Carovillano, The National Space Weather Program: Strategic Plan, FCM-P30-1995, Washington, DC, 1995.

Brekke, A., C. Hall, and T. L. Hansen, Auroral ionospheric conductances during disturbed conditions, *Ann. Geophysicae, 7*, 269, 1989.

Kelly, J. D., C. J. Heinselman, J. F. Vickrey, and R. R. Vondrak, The Sondrestrom radar and accompanying ground-based instrumentation, *Space Sci. Rev., 71,* 797, 1995.

Lummerzheim, D., M. H. Rees, D. J. Craven, and L. A. Frank, Ionospheric conductances derived from DE-1 auroral images, *J. Atm. Terr. Phys., 53,* 281, 1991.

Min, Q.-L., D. Lummerzheim, M. H. Rees, and K. Stamnes, Effects of a parallel electric field and the geomagnetic field in the topside ionosphere on auroral and photoelectron energy distributions, *J. Geophys. Res., 98,* 19223, 1993.

Press, W. H., B. P. Flannery, S. A. Teukolsky and W. T. Vetterling, *Numerical Recipes,* 655-659 pp., Cambridge University Press, Cambridge, 1989.

Rees, M. H., *Physics and Chemistry of the Upper Atmosphere*, pp. 39-42, Cambridge University Press, Cambridge, 1989.

Robinson, R., R. R. Vondrak, J. D. Craven, L. A. Frank, and K. Miller, A comparison of ionospheric conductances and auroral luminosities observed simultaneously with the Chatanika radar and the DE 1 auroral imagers, *J. Geophys. Res., 94,* 5382, 1989.

Robinson, R., T. Dabbs, J. Vickrey, R. Eastes, F. del Greco, R. Huffman, C. Meng, R. Daniell, D. Strickland, and R. Vondrak, Coordinated measurements made by the Sondrestrom radar and the Polar Bear ultraviolet imager, *J. Geophys. Res., 97,* 2863, 1992.

Stolarski, R. S., Calculation of auroral emission rates and heating effects, *Planet. Space Sci., 16,* 1265, 1968.

Torr, M. R., D. G. Torr, M. Zukic, R. B. Johnson, J. Ajello, P. Banks, K. Clark, K. Cole, C. Keffer, G. Parks, B. Tsurutani, and J. Spann, A far ultraviolet imager for the International Solar-Terrestrial Physics mission, *Space Sci. Rev., 71,* 329, 1995.

Vickrey, J. F., R. R. Vondrak, and S. J. Matthews, Energy deposition by precipitating particles and joule dissipation in the auroral ionosphere, *J. Geophys. Res., 87,* 5184, 1982.

Vondrak, R. R., and M. J. Baron, A method of obtaining the energy distribution of auroral electrons from incoherent scatter radar measurements, *Radar Probing of the Auroral Plasma*, pp. 103-144, Universitetsforlaget, Tromsø-Oslo-Bergen, 1977.

R. A. Doe and J. D. Kelly, SRI International, 333 Ravenswood Avenue, Menlo Park, CA 94025. (e-mail: doe@unix.sri.com; kelly@sri.com)

D. Lummerzheim, University of Alaska, Fairbanks, AK 99775-7320. (e-mail: lumm@odin.gi.alaska.edu)

G. Parks and M. J. Brittnacher, University of Washington, Box 351650, Seattle, WA 98195.

G. A. Germany, University of Alabama, Optical Aeronomy Laboratory, Rm 348, Huntsville, AL 35899.

J. Spann, Space Science Laboratory, Marshall Space Flight Center, Huntsville, AL 35812.

(Received October 14, 1996; revised February 3, 1997; accepted February 3, 1997.)